

SCIENTIFIC REPORTS



OPEN

Novel Hybrid Evolutionary Algorithms for Spatial Prediction of Floods

Received: 11 April 2018
Accepted: 6 October 2018
Published online: 18 October 2018

Dieu Tien Bui^{1,2}, Mahdi Panahi³, Himan Shahabi⁴, Vijay P. Singh⁵, Ataollah Shirzadi⁶, Kamran Chapi⁶, Khabat Khosravi⁷, Wei Chen⁸, Somayeh Panahi⁹, Shaojun Li¹⁰ & Baharin Bin Ahmad¹¹

Adaptive neuro-fuzzy inference system (ANFIS) includes two novel GIS-based ensemble artificial intelligence approaches called imperialistic competitive algorithm (ICA) and firefly algorithm (FA). This combination could result in ANFIS-ICA and ANFIS-FA models, which were applied to flood spatial modelling and its mapping in the Haraz watershed in Northern Province of Mazandaran, Iran. Ten influential factors including slope angle, elevation, stream power index (SPI), curvature, topographic wetness index (TWI), lithology, rainfall, land use, stream density, and the distance to river were selected for flood modelling. The validity of the models was assessed using statistical error-indices (RMSE and MSE), statistical tests (Friedman and Wilcoxon signed-rank tests), and the area under the curve (AUC) of success. The prediction accuracy of the models was compared to some new state-of-the-art sophisticated machine learning techniques that had previously been successfully tested in the study area. The results confirmed the goodness of fit and appropriate prediction accuracy of the two ensemble models. However, the ANFIS-ICA model (AUC = 0.947) had a better performance in comparison to the Bagging-LMT (AUC = 0.940), BLR (AUC = 0.936), LMT (AUC = 0.934), ANFIS-FA (AUC = 0.917), LR (AUC = 0.885) and RF (AUC = 0.806) models. Therefore, the ANFIS-ICA model can be introduced as a promising method for the sustainable management of flood-prone areas.

Flood is considered as one of the most destructive natural disasters worldwide, because of claiming a large number of lives and incurring extensive damage to the property, disrupting social fabric, paralyzing transportation systems, and threatening natural ecosystems^{1,2}. Each year flooding affects around 200 million people and causes economic losses of about \$95 billion around the world³. In Asia, more than half of flood damages are economic and over 90% of all human casualties are the result of flood occurrence⁴. Iran has witnessed many devastating floods recently, especially in the northern cities of Noshahr (2012), Neka (2013), Behshahr (2013), and Sari (2015), all located in the Haraz watershed⁵, Mazandaran, Iran. Arable lands of 28 villages with an area of 80 ha had been destroyed in Chahardangeh district, Sari city; Also, 150 hectares of agricultural lands were degraded in Klijan Restagh in the same city located in the study area⁵.

Although flood prediction models can be used for evaluation of floods that have occurred in the region, prevention of flooding may not be completely possible due to its complexity⁶. Hence, an important solution to reduce future flood damages is to develop models for flood susceptibility mapping based on the determination of

¹Geographic Information Science Research Group, Ton Duc Thang University, Ho Chi Minh City, Vietnam. ²Faculty of Environment and Labour Safety, Ton Duc Thang University, Ho Chi Minh City, Vietnam. ³Geohazard Department Manager, Samaneh Kansar Zamin (SKZ) Company, Tehran, Iran. ⁴Department of Geomorphology, Faculty of Natural Resources, University of Kurdistan, Sanandaj, Iran. ⁵Department of Biological and Agricultural Engineering & Zachry Department of Civil Engineering, Texas A & M University, College Station, TX, 77843-2117, USA. ⁶Department of Rangeland and Watershed Management, Faculty of Natural Resources, University of Kurdistan, Sanandaj, Iran. ⁷Department of Watershed Management, Faculty of Natural Resources, Sari Agricultural Science and Natural Resources University, Sari, Iran. ⁸College of Geology & Environment, Xi'an University of Science and Technology, Xi'an, 710054, Shaanxi, China. ⁹Young Researchers and Elites Club, North Tehran Branch, Islamic Azad University, Tehran, Iran. ¹⁰State Key Laboratory of Geomechanics and Geotechnical Engineering, Institute of Rock and Soil Mechanics, Chinese Academy of Sciences, Wuhan, Hubei, 430071, China. ¹¹Department of Geoinformation, Faculty of Geoinformation and Real Estate, Universiti Teknologi Malaysia (UTM), Johor Bahru, Malaysia. Correspondence and requests for materials should be addressed to H.S. (email: h.shahabi@uok.ac.ir)

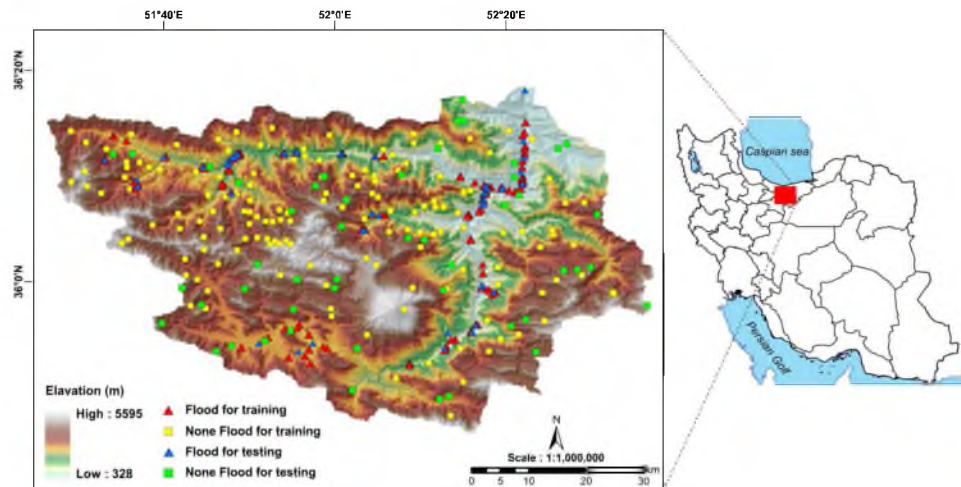


Figure 1. Geographical situation of Haraz watershed and locations of flood and non-flood occurrences in the study area.

flood-prone regions^{5,7}. Furthermore, flood susceptibility maps can display the potential of regions for developmental activities by categorizing the sensitivity of areas to flooding⁸.

Recently, some researchers have studied flood susceptibility mapping (FSM) by Remote Sensing (RS) techniques and GIS using different conventional and statistical models, including frequency ratio (FR)⁹, logistic regression (LR)¹⁰, spatial multi-criteria evaluation (SMCE)¹¹, analytical hierarchy processes (AHP)¹², weight of evidence (WOE)¹³, and evidential belief functions (EBF)¹⁴. In this regard, Cao *et al.*¹⁵ compared the FR and statistical index (SI) approaches for flood modelling in the Xiqu Gully (XQG) of Beijing, China¹⁵. They found that the FR was more powerful in comparison to the SI method for spatial prediction of floods. Tehrany *et al.* (2017) observed that the WOE method outperformed the LR and FR methods. In addition to the above-mentioned models, recently, various machine learning approaches and their ensembles have also been applied to FSM including neuro-fuzzy¹⁶, artificial neural networks^{17,18}, support vector machines¹⁹, Shannon entropy²⁰, decision trees²¹, Naive Bayes²², random forest (RF)²³, and logistic model tree^{3,21}. Chapi *et al.*³ introduced a new hybrid artificial intelligence method called Bagging-logistic model tree (LMT) for flood mapping in Haraz watershed, Iran. They also compared the results of the new proposed model with several soft computing benchmark models including LR, Bayesian logistic regression (BLR), and RF. Their results indicated that the new proposed model outperformed and outclassed the other models. Additionally, the results revealed that the prediction accuracy of BLR was greater than that of the LMT, LR and RF models³. Khosravi *et al.*²¹ compared some decision tree algorithms including LMT, Reduced Error Pruning Trees (REPT), NBT, and alternating decision tree (ADTree) for flood mapping in Haraz watershed²¹. The results suggested that the ADTree was a more powerful and robust algorithm compared to the NBT, LMT and REPT algorithms. Overall, these results of literature indicated that, one the one hand, the results of performance of all conventional, statistical and machine learning methods are different from a region to another due to the different geo-environmental factors. On the other hand, the results of flood modelling in a given region are also different for some models. This is due to the difference in the structure and framework of the applied algorithms. Therefore, finding the most appropriate model for detecting the flood-prone areas through comparing different methods and also proposing a new model for every region is of great interest to environmental researchers. Among recent approaches on flood, ANFIS model which is a combination of ANN and fuzzy logic, has become increasingly popular^{16,24}. However, in some cases, it has not been able to predict the best weights in the modelling process²⁵. Therefore, to address this challenge, it is better to use some evolutionary/optimization algorithms enabling us to re-weigh in order to obtain the maximum performance. Although there are some optimization algorithms with different structures and probability distribution functions (PDF) to find the best weights, selecting the best algorithm for the modelling process is a critical issue in the spatial prediction of natural hazard events such as floods. Hence, new hybrid algorithms should be examined to find the best weights and obtain more reasonable results. In this regard, the current study uses new hybrid algorithms including ANFIS-ICA and ANFIS-FA for spatial prediction of floods in Haraz watershed in the northern part of Iran. Although some optimization and machine learning algorithms have been applied to flood modelling around the world, our optimization methods have not been previously explored for flood assessment. For validation and comparison, several quantitative methods such as the Receiver Operating Characteristic (ROC) curve method as well as statistical analysis methods were selected. Computations were performed using Matlab 2016a and ArcGIS 10.2 software.

Description of the Study Area

Located between longitudes of 51° 43' to 52° 36'E, and latitude of 35° 45' to 36° 22'N, Haraz watershed is situated in the south of Amol City in Mazandaran Province, Northern Iran. This watershed drains an area of 4,014 km². Elevation of the watershed ranges from 328 m to about 5595 m at the highest point and its ground slope varies from flat to 66° (Fig. 1). The average annual rainfall is around 770 mm. The maximum rainfall occurs in January,



Figure 2. Flood damages in Haraz watershed during recent years, Mazandaran Province taken from field surveys by the sixth author (K. K.).

February, March, and October with an average monthly rainfall of 160 mm (Iran's Meteorological Organization) during these four months. The climate in the study area is a combination of the mild humid climate of the Caspian shoreline area and the moderate cold climate of mountainous regions. The area is almost entirely encompassed by rocks from Mesozoic (56.4%), Cenozoic (38.9%), and Paleozoic (4.7%) eras. The rangeland covers around 92% of the study area. Other land use patterns present in the area include forest, irrigation land, bare land, garden land, and residential area.

The main residential centres located in Haraz watershed include Abasak, Baladeh, Gaznak, Kandovan, Noor, Polur, Rineh, Tashal, and Tiran⁵. The Haraz watershed was considered for the present study due to the many devastating floods that have occurred annually, claiming lives and incurring damage to the property in recent years. The major reason for flooding in these areas is high rainfall intensity within a short period of time, major land use changes specifically from rangelands to farmlands, deforestation, recent extensive changes from orchards to residential areas, and the lack of control measures required to curb flooding. In the study area, floods lead to fatalities and damages to infrastructure, and disruption of traffic, trade and public services (Fig. 2).

Results and Discussion

Spatial relationship between floods and influential factors using SWARA model. The first step in this study was determining the sub-factor weights based on the SWARA algorithm, as presented in Table 1. In this study, 10 factors showing a significant impact on flood occurrence were selected based on literature review, the characteristics of watershed, and data availability⁵. One of the most significant factors in flood modelling is the slope angle. The slope map was developed and then classified into seven classes by the natural break classification method. The SWARA value was the highest for the class 0–0.5 (0.4). Hence, the results revealed that the higher the slope angle, the less the probability of flooding will be. Another important factor was elevation which was classified into nine classes. The results showed that the first class, 328–350 m, with a weight of 0.63, had the highest impact on flooding such that the higher the elevation, the lower the flooding probability will be. This was confirmed by Khosravi *et al.*⁵ and Tehrany *et al.*¹⁹ who explained that slope angle, elevation, and distance to river had higher impacts on flooding such that once the slope angle, elevation, and distance to river increased, the probability of flooding diminished. Meanwhile, curvature is representative of topography of the ground surface. This factor was prepared and classified into three classes including concave, convex, and flat. For curvature, the highest SWARA value was found for concave followed by flat and convex.

The results of SPI revealed that the class of 2000–3000 (0.32) showed a higher impact on flood occurrence than other classes such that higher SPIs were associated with higher flood probability. In the case of topographic wetness index (TWI), the SWARA value showed a decreasing trend when the TWI value increased. The highest SWARA value belonged to the class of 6.96–11.5 (0.08). TWI indicates the wetness of land; wetness was higher in areas with lower slope than mountainous areas. This suggests that larger TWI values are associated with higher

Factors	Classes	Comparative importance of average value K_j	Coefficient $K_j = S_j + 1$	$w_j = (X_{(j-1)})/k_j$	weight $w_j / \text{sigma } w_j$
Slope	0–0.5	—	1.00	1.00	0.40
	0.5–2	0.80	1.80	0.56	0.22
	2–5	0.20	1.20	0.46	0.18
	5–8	0.60	1.60	0.29	0.11
	8–13	1.15	2.15	0.13	0.05
	13–20	1.50	2.50	0.05	0.02
	>30	2.70	3.70	0.01	0.01
	20–30	0.55	1.55	0.01	0.00
Elevation	328–350	—	1.00	1.00	0.63
	400–450	3.70	4.70	0.21	0.13
	350–400	0.35	1.35	0.16	0.10
	450–500	0.55	1.55	0.10	0.06
	500–1000	0.65	1.65	0.06	0.04
	1000–2000	3.95	4.95	0.01	0.01
	2000–3000	0.00	1.00	0.01	0.01
	3000–4000	0.00	1.00	0.01	0.01
4000>	0.00	1.00	0.01	0.01	
Curvature	Concave	—	1.00	1.00	0.46
	Flat	0.05	1.05	0.95	0.43
	Convex	3.00	4.00	0.24	0.11
SPI	2000–3000	—	1.00	1.00	0.32
	800–2000	0.10	1.10	0.91	0.29
	400–800	0.30	1.30	0.70	0.22
	80–400	0.70	1.70	0.41	0.13
	0–80	3.70	4.70	0.09	0.03
	>3000	3.95	4.95	0.02	0.01
TWI	6.96–11.5	—	1.00	1.00	0.08
	5.72–6.96	0.10	1.10	0.91	0.07
	5.03–5.72	0.65	1.65	0.55	0.04
	4.47–5.03	2.70	3.70	0.15	0.01
	3.94–4.47	3.50	4.50	0.03	0.00
	1.9–3.94	0.05	1.05	0.03	0.00
River density	2.67–3.66	—	1.00	1.00	0.00
	3.66–7.3	0.00	1.00	1.00	0.01
	1.92–2.67	0.85	1.85	0.54	0.06
	1.17–1.92	2.50	3.50	0.15	0.20
	0.401–1.17	3.95	4.95	0.03	0.37
	0–0.401	3.95	4.95	0.01	0.37
Distance to river	0–50	—	1.00	1.00	0.59
	50–100	1.75	2.75	0.36	0.22
	100–150	0.85	1.85	0.20	0.12
	150–200	1.20	2.20	0.09	0.05
	200–400	2.70	3.70	0.02	0.01
	400–700	2.70	3.70	0.01	0.00
	700–1000	3.00	4.00	0.00	0.00
	>1000	0.00	1.00	0.00	0.00
Lithology	Teryas	—	1.00	1.00	0.31
	Quaternary	0.50	1.50	0.67	0.21
	Permain	0.00	1.00	0.67	0.21
	Cretaceous	0.40	1.40	0.48	0.15
	Jurassic	1.10	2.10	0.23	0.07
	Teratiary	0.10	1.10	0.21	0.06
Continued					

Factors	Classes	Comparative importance of average value K_j	Coefficient $K_j = S_j + 1$	$w_j = (X_{(j-1)})/k_j$	weight $w_j / \text{sigma } w_j$
Land use	Water bodies	—	1.00	1.00	0.75
	Residential area	3.90	4.90	0.20	0.15
	Garden	1.55	2.55	0.08	0.06
	Forest land	2.00	3.00	0.03	0.02
	Grassland	0.70	1.70	0.02	0.01
	Farming Land	3.95	4.95	0.00	0.00
	Barren land	0.00	1.00	0.00	0.00
Rainfall	188–333	—	1.00	1.00	0.40
	379–409	1.20	2.20	0.45	0.18
	409–448	0.35	1.35	0.34	0.13
	333–379	0.10	1.10	0.31	0.12
	448–535	0.05	1.05	0.29	0.12
	535–471	1.15	2.15	0.14	0.05

Table 1. Spatial relationship between flood and conditioning factors of SWARA model.

		Slope angle	Elevation	Curvature	TWI	SPI	Rainfall	Dis-river	River density	Lithology	Land use	All
ANFIS-ICA	Train	0.067	0.065	0.076	0.074	0.089	0.053	0.066	0.076	0.044	0.048	0.069
	Test	0.196	0.141	0.172	0.145	0.133	0.143	0.134	0.172	0.145	0.134	0.130
ANFIS-FA	Train	0.084	0.080	0.094	0.075	0.078	0.063	0.080	0.081	0.052	0.059	0.078
	Test	0.269	0.196	0.257	0.193	0.173	0.198	0.171	0.260	0.201	0.171	0.170

Table 2. Sensitivity analysis of flood modeling using ANFIS-ICA and ANFIS-FA models.

flood probability. River density results also showed that the river density values higher than 3.66 had the highest correlation with flood occurrence (0.37). The results of the SWARA model revealed that as the river density grew, the probability of flood occurrence also increased. For distance-to-river factor, the results demonstrated that the first class of 0–50 m (0.59) had a relatively higher susceptibility to flood occurrence. The farther the distance to the river, the less probable the flood occurrence was. For lithology, Teryas formations had the highest SWARA value (0.31) suggesting the highest probability of flood occurrence.

The land use map was constructed for seven types including water bodies, residential area, garden, forest land, grassland, farming land, and barren land. The water bodies demonstrated a higher impact on flood occurrence (0.75), followed by residential area (0.15), garden (0.06), forest land (0.02), grassland (0.01), farming land (0), and barren land (0). The highest SWARA value (0.4) was assigned to the lowest amount of rainfall (188–333), where the higher the rainfall level, the less the flood occurrence probability was. The reason why rainfall increase was still insignificant for flooding was that rainfall increased in areas where elevation increased and these areas were not prone to flooding⁵.

Sensitivity analysis of conditioning factors. The results of sensitivity analysis are reported in Table 2. Based on the testing error values, the results indicated that in the ANFIS-ICA hybrid model, when the slope angle, elevation, curvature, TWI, SPI, rainfall, distance to river, river density, lithology, and land use were removed, the RMSE values were 0.196, 0.141, 0.172, 0.145, 0.133, 0.143, 0.134, 0.172, 0.145, and 0.134, respectively. It was observed that when all factors were considered in the modelling process, the error value was 0.130. It was also seen that all conditioning factors had a positive role in the flood modelling process. On the other hand, the results of sensitivity analysis for ANFIS-FA hybrid model concluded that with removing the slope angle, elevation, curvature, TWI, SPI, rainfall, distance to river, river density, lithology, and land use factors, the RMSE values were computed as 0.269, 0.196, 0.257, 0.193, 0.173, 0.198, 0.171, 0.260, 0.201, and 0.171, respectively. In this model, when all factors were introduced into the model, the error value was 0.170. Overall, the results suggested that all factors were also significant for flood modelling in ANFIS-FA hybrid model.

Application of ANFIS ensemble models. Using the MATLAB programming language, two hybrid models called ANFIS with complementary models of FA and ICA were developed, leading to ANFIS-ICA and ANFIS-FA, which were initially trained. The accuracy of training was then calculated using test data. To that end, the dataset related to flood and non-flood was segmented into 70% for training and 30% for testing. Then, the two methods started extracting and learning the relationship between the SWARA values for conditioning factors and flood (1) as well as non-flood (0) values.

Model results and validation. The results of the model prediction capacity were evaluated using Mean Squared Error (MSE) and Root Mean Squared Error (RMSE) for both modelling and validation²⁵. Figures 3 and 4 demonstrate the comparison between the training dataset as a target and estimated flood pixels as the output for modelling by ANFIS-ICA and ANFIS-FA. The MSE and RMSE values for ANFIS-ICA and ANFIS-FA models

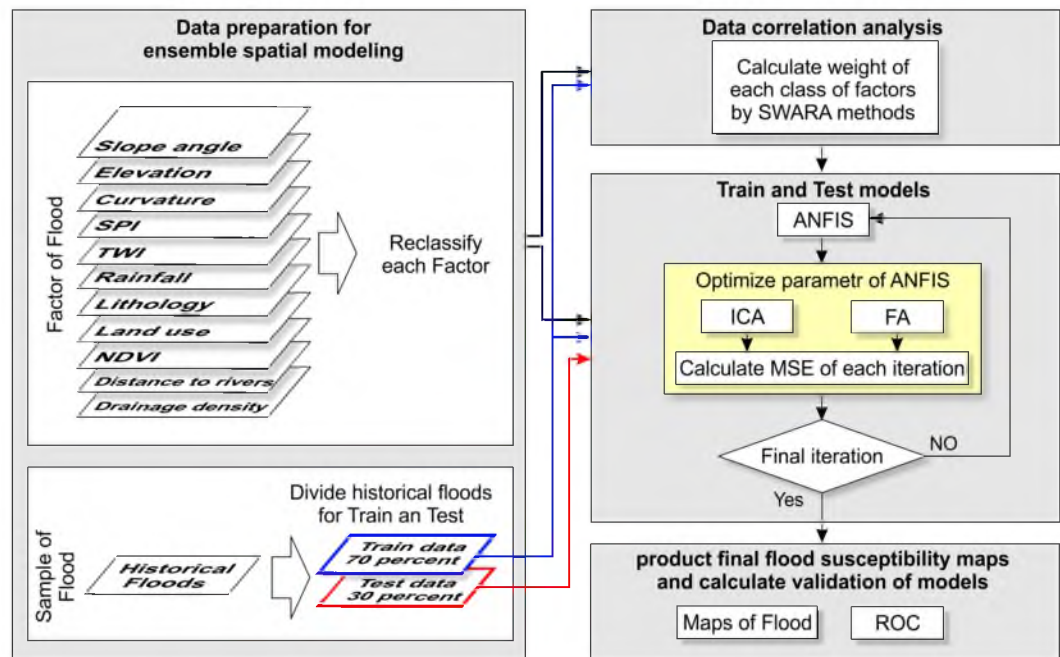


Figure 3. ANFIS-ICA model. (a) Target and output ANFIS-ICA value of the training data samples; (b) MSE and RMSE value of the training data samples; (c) frequency errors of the training data samples; (d) target and output ANFIS-ICA value of the testing data samples; (e) MSE and RMSE value of the testing data samples; and (f) frequency errors of the testing data samples.

were 0.069 and 0.26 in the training, and 0.078 and 0.27 in the testing, respectively. Accordingly, ANFIS-ICA had a better performance compared to ANFIS-FA in the training due to lower MSE and RMSE. Note that the optimized model was the model that predicted the results of testing data with higher accuracy. The values of MSE and RMSE for ANFIS-ICA and ANFIS-FA were obtained as 0.41 and 0.35, and 0.169 and 0.129, respectively. Since MSE and RMSE of ANFIS-ICA were lower than of those of ANFIS-FA, it can be concluded that ANFIS-ICA was a more optimal model than ANFIS-FA, since ANFIS-ICA had higher accuracy in both the training and testing.

Preparation of flood susceptibility mapping using ANFIS ensemble models. In this study, the ensembles of ANFIS based on the ICA and FA algorithms were developed by the training dataset. The developed models were then applied for calculating the flood susceptibility index (FSI) which was assigned to all pixels of the study area to create flood susceptibility maps (FSM). In the first step, each pixel of the study area was assigned to a unique flood susceptibility index; then, these indices were exported in Arc GIS 10.2 format and used to construct the final flood susceptibility mapping.

There are different techniques for map classification in the Arc GIS 10.2 software including natural break, equal interval, geometrical interval, quantile, standard deviation, and even manual technique. They should be tested to select the most appropriate one to classify any map in the study area. Generally, selection of the classification methods is based on the distribution of flood susceptibility indexes²⁶. For example, if the distribution of FSI values is close to normal, to prepare an equal interval, FSM or standard deviation classification methods should be used. However, when FSI has positive or negative skewness, the best classification methods are quantile or natural break²⁷. In the current study, the data distribution histogram revealed that quantile classifier was capable of generating better results compared to other classifiers. Thus, the approach of quantile data classification was selected, and FSI was classified in four classes of susceptibility: low, moderate, high, and very high¹⁹. Finally, based on the hybrid model, the two maps of flood susceptibility were constructed, as depicted in Figs 5 and 6.

Validation and comparison of new hybrid flood susceptibility models. *Validation of the proposed ensemble models.* The reliability and predictive power of these two new hybrid models for flood modelling were assessed using success and prediction rate curves. The outcomes of success and prediction rate were prepared for 70% (training data) and 30% (testing data that were not used in training) of data. Since the success rate curve was drawn using the training data, it was impossible to evaluate the predictive power of the models²⁸. On the other hand, the AUC for prediction rate curve showed how well the model predicted floods²⁹. The area under ROC curve was considered for evaluating the overall performance of the models. According to that, Larger AUC represented better performance of the model. The ROC method has been one of the most popular techniques to evaluate the efficiency of models, as this method quantitatively calculates the efficiency of models⁵. The results of success-rate showed that the AUC values for the two models of ANFIS-ICA and ANFIS-FA were 0.95 and 0.93, respectively (Fig. 7a). The prediction rate which was not used in the modelling was applied to the assessment of the model capacity in predicting flood-prone areas. The values of area under the prediction-rate curve for

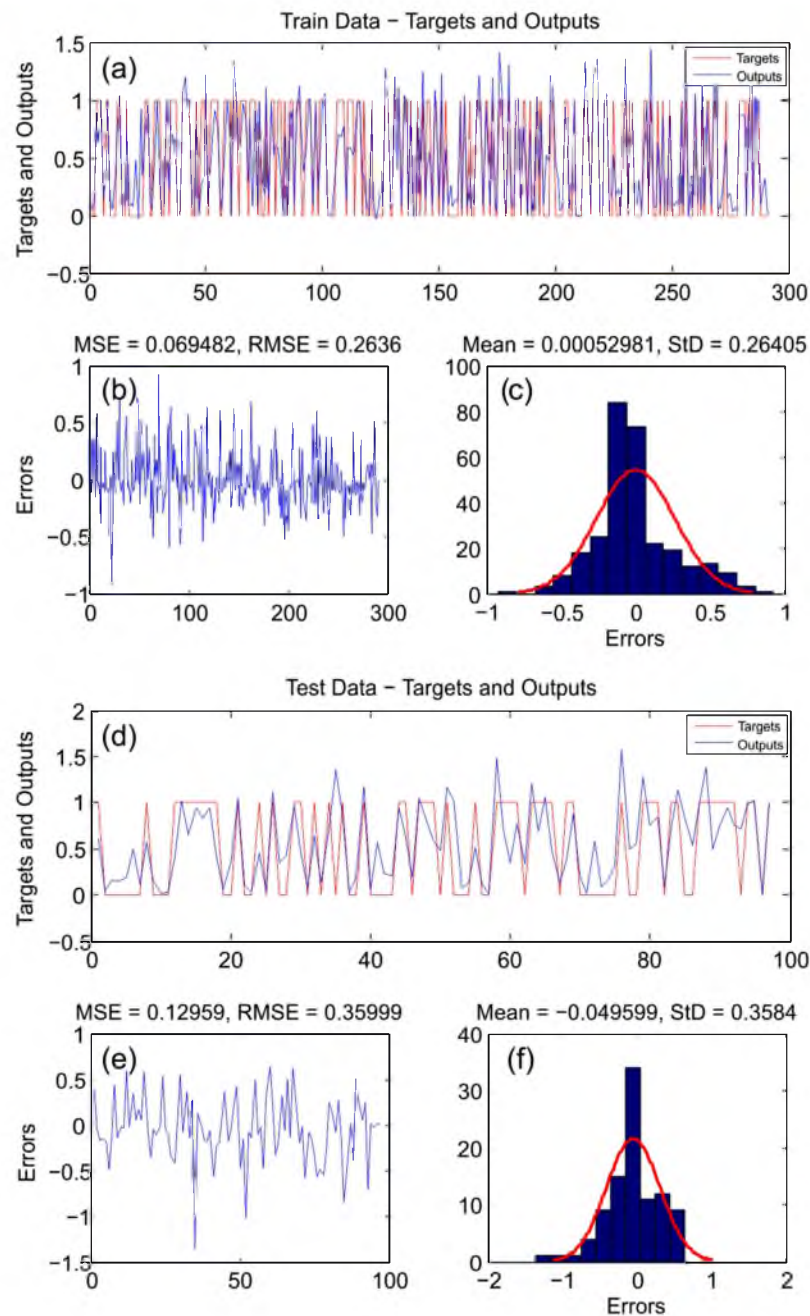


Figure 4. ANFIS-FA model. (a) Target and output ANFIS-FA value of the training data samples; (b) MSE and RMSE value of the training data samples; (c) frequency errors of training the data samples; (d) target and output ANFIS-FA value of the testing data samples; (e) MSE and RMSE value of the testing data samples; and (f) frequency errors of the testing data samples.

ANFIS-ICA and ANFIS-FA were 0.94 and 0.91, respectively (Fig. 7b). Then, the highest predictive power for flood-prone areas in the Haraz watershed was provided by the new hybrid ANFIS-ICA model, which had also a lower standard error of 0.35 compared to the ANFIS-FA (0.41) model. The results were compatible with those of the RMSE and MSE values in both the training and testing phases. These two new hybrid models had also a reasonable ROC; yet, the ANFIS-ICA model represented the best performance in predicting the flood susceptibility, followed by the ANFIS-FA model.

In addition to the success and prediction rate curves, Friedman and Wilcoxon signed-rank tests were also utilized for assessing the validity of the two new hybrid models (the performance of the models). They determined whether there were significant statistical differences between performances of the two hybrid models. The results of Friedman test reported in Table 3 indicated that the average ranking values for the ANFIS-ICA and ANFIS-FA hybrid models were 1.29 and 1.71, respectively. Although chi-square value was 35.945, due to having a significant level of less than 5%, the Friedman test was not applicable to assess the validity of models.

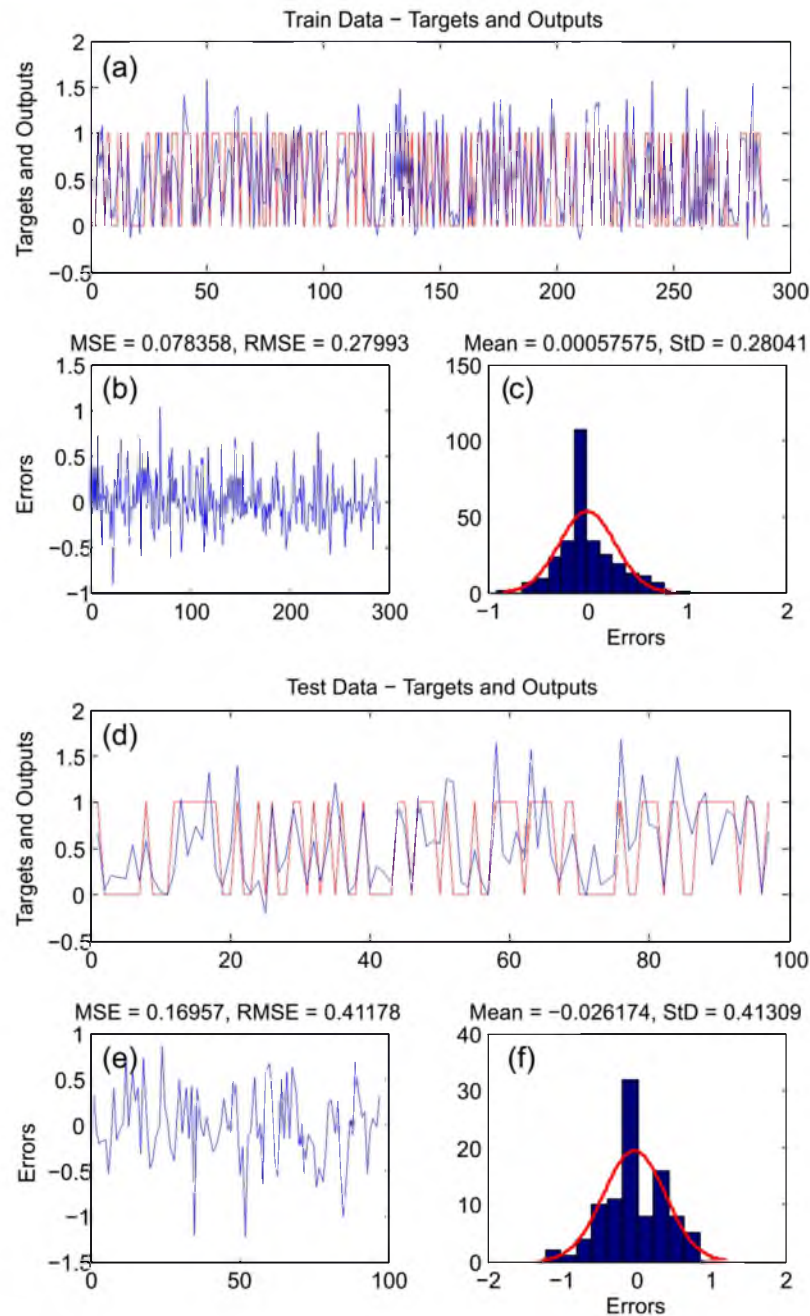


Figure 5. Flood susceptibility mapping prepared via ANFIS-ICA model.

To overcome this challenge, the Wilcoxon signed-rank test was performed for determining the pairwise differences between the two flood hybrid models at the 5% significance level (Table 4). No significant difference was detected between the two flood hybrid models at the significance level of 5% when the null hypothesis was rejected. On the other hand, in this case their results were not the same. The results of Wilcoxon signed-rank test were specified based on the p-value and z-value. If the p-value was less than 5% (0.05), and z-value was larger than -1.96 and $+1.96$, the performances of the two models were significantly different³⁰. The results of Wilcoxon signed-rank test, shown in Table 3, imply that there was a statistical difference between the two flood susceptibility models.

Comparison with some state-of-the-art sophisticated machine learning techniques. Chapi *et al.*³ introduced a novel ensemble data mining model called Bagging-logistic model tree (LMT) for mapping of flood susceptibility in this study area. Then, the results of this new model were compared with those of some state-of-the-art sophisticated machine learning models including LMT, Bayesian logistic regression (BLR), logistic regression (LR) and random forest (RF). Comparison in Fig. 8 reveals that the new proposed model outperformed all these models. For the validation dataset, the highest AUC was obtained for the new ensemble model ($AUC_{\text{Bagging-LMT}} = 0.940$),

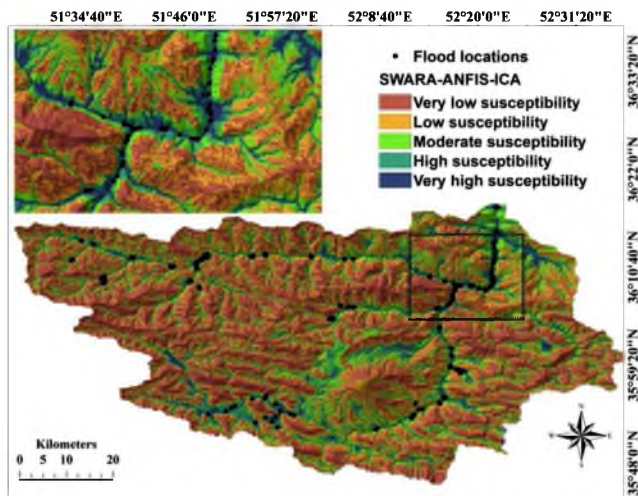


Figure 6. Flood susceptibility mapping prepared by ANFIS-FA model.

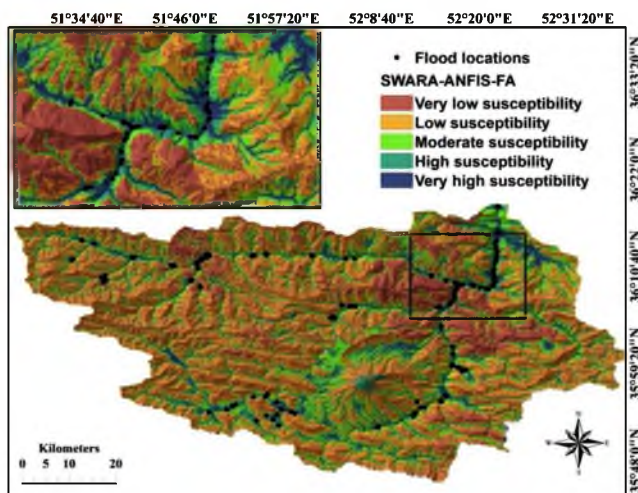


Figure 7. Area under the curves of success rate (a) and prediction rate (b) of new flash flood hybrid models.

No	Flash flood models	Mean ranks	χ^2	Sig.
1	ANFIS-ICA	1.29	35.945	0.000
2	ANFIS-FA	1.71		

Table 3. Average ranking of the two flash flood susceptibility hybrid models using Friedman’s test.

No	Pair wise comparison	Number of positive differences	Number of negative differences	z-value	p-value	Significance
1	S-A-ICA vs. S-A-FA	143	58	-3.982	0.000	Yes

Table 4. Performance of the new flash flood hybrid models by Wilcoxon signed-rank test (two-tailed). (The standard p value is 0.05).

followed by BLR (AUC = 0.936), LMT (AUC = 0.934), LR (AUC = 0.885) and RF (AUC = 0.806). The evolutionary algorithm, ANFIS-ICA (AUC = 0.947) outperformed all these models, but ANFIS-FA was unable to show a greater performance than the Bagging- LMT, BLR and LMT models. However, AUC_{ANFIS-FA} was better than the LR and RF models. Overall, the new proposed model, ANFIS-ICA, was a powerful ensemble model which improved the prediction accuracy among all models in this study area.

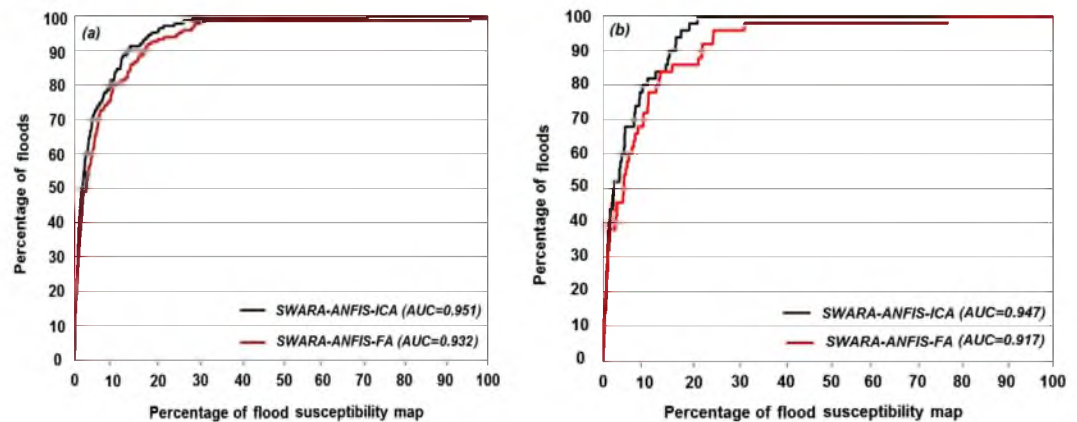


Figure 8. Area under curve of the prediction rate using validation dataset.

Conclusions

The dynamic nature of floods will always necessitate new approaches and models for its management. This is the main reason that no one has been able to introduce the best model. Unpredicted spatial-temporal changes of this phenomenon have forced scientists to continuously seek for better approaches to generate better results and outcomes; sometimes new individual models and sometimes combinations of the individual models known as hybrid models. In the current study, two new hybrid models, ANFIS-ICA and ANFIS-FA, were applied to enhance the predictive power of flood spatial modelling. A total of 10 conditioning factors were selected for the spatial modelling in the Haraz watershed, Northern Iran. The factors were divided into several classes using the SWARA model and their maps were generated for modelling purposes. The new hybrid models were then used for modelling spatial floods in the study area. The models' outputs were compared to the results of several soft computing approaches that had been successfully used before in the study area whose accuracy had been approved. The ANFIS-ICA model was the most successful among all the models and its results provided the most appropriate congruence with reality. Although the results of ANFIS-FA were reasonable, the model was not ranked as the best. Accordingly, this study introduced a new model, ANFIS-ICA, for spatial prediction of floods in the study area and other similar watersheds. This model can be evaluated as a tool for more appropriate mitigation and management of floods in Northern Iran.

Materials and Methods

Data collection and preparation. Flood inventory maps, which are generated in accordance with historical flood data, are the cornerstones of spatial prediction of floods. The quality of historical data is closely related to the accuracy of the prediction model³¹. Combined with field survey, flood records in 2004, 2008 and 2012 were employed to develop a flood inventory map for the study area. Additionally, DEM and geological maps in the Haraz watershed were also used in data collection and preparation. Eventually, 201 flood points and non-flood points were selected utilizing satellite images. In order to build spatial prediction models and to test the validity of model results, these data points were randomly divided into a training (70%; 141 locations) and a testing (30%; 60 locations) set³. In the present study, 10 flood conditioning factors were adopted: curvature, distance to river, elevation, land use, lithology, rainfall, river density, SPI, slope, and TWI. These factors were extracted using DEM and geological maps by ArcGIS software.

Sensitivity analysis. The relative importance of different conditioning factors affecting the modelling process and outputs should be assessed using sensitivity analysis approaches^{32,33}. Iliä and Tsangaratos (2016) reported that the sensitivity analysis is performed using three methods including: (i) Changing criteria values, (ii) Changing relative importance of criteria, and (iii) Changing criteria weights³⁴. The current study adopted the second method, changing relative importance of criteria, such that each conditioning factor was firstly removed and then modelling was performed with other factors. Accordingly, the obtained results were compared with the condition taking all conditioning factors for the modelling into account by error estimation such as RMSE measure.

Theoretical background of the methods used. *Stepwise Assessment Ratio Analysis (SWARA).* The Step-wise Assessment Ratio Analysis (SWARA), which was first proposed by Keršulienė in 2010, is one of the Multi-Criteria Decision Making (MCDM) methods. Experts play an important part in calculating the weights in this method, and hence the SWARA method is called an expert-oriented method³⁵. The expert assigns the highest rank to the most valuable and the lowest rank to the least valuable criteria. Subsequently, the average value of these ranks determines the overall ranks. The SWARA method follows these steps³⁵:

Step 1: Criteria are developed and determined. The expert must develop decision-making models from the determined factors. Moreover, the criteria are arranged in accordance with their priority and the importance assigned by the expert's viewpoint and then the influential criteria are sorted in a descending order.

Step 2: criteria's weighting is calculated. Then, the weights are assigned to all criteria based on expert's knowledge, information gained for the case study, and the previous experience as follows:

The respondent expresses the comparative importance of the criterion j compared to the previous $(j - 1)$ criterion starting from the second criterion, with the trend repeating the same way for each particular criterion. The trend, according to Keršulienė, determines the relative importance of the average value, S_j in this manner³⁵:

$$S_j = \frac{\sum_i^n A_i}{n} \quad (1)$$

where, n represents the number of experts; A_i stands for the ranks suggested by the experts for each factor; and j shows the number of factors involved. The coefficient K_j is calculated as:

$$K_j = \begin{cases} 1 & j = 1 \\ S_j + 1 & j > 1 \end{cases} \quad (2)$$

The recalculation of Q_j is done by:

$$Q_j = \frac{X_{j-1}}{K_j} \quad (3)$$

The relative weights of evaluation criteria can be expressed as:

$$W_j = \frac{Q_j}{\sum_{j=1}^m Q_j} \quad (4)$$

where, W_j denotes the relative weight of the j -th criterion, and m represents the total number of criteria.

Adaptive neuro-fuzzy inference systems (ANFIS). Adaptive Neuro Fuzzy Inference System (ANFIS) is a data-driven model belonging to the family of neuro-fuzzy methods. The ANFIS is a hybrid algorithm integrating neural network with fuzzy logic which generates input-output data pairs³⁶. This algorithm, first proposed by Jang in³⁷, is used in many fields such as data processing of landslides³⁸, flooding²⁵, and groundwater³⁹. The fuzzy inference system has two inputs x_1 and x_2 , one output z , the fuzzy set A_1, A_2, B_1, B_2 , and p_i, q_i , and r_i which are the consequence of output function parameters in a set of fuzzy IF-THEN rules based on the first-order Takagi-Sugeno fuzzy model⁴⁰ as follows:

$$\text{Rule 1: if } x_1 \text{ is } A_1 \text{ and } y_1 \text{ is } B_1, \text{ then } f_1 = p_1 x_1 + q_1 y_1 + r_1 \quad (5)$$

$$\text{Rule 1: if } x_2 \text{ is } A_2 \text{ and } y_2 \text{ is } B_2, \text{ then } f_2 = p_2 x_2 + q_2 y_2 + r_2 \quad (6)$$

The ANFIS is a feedforward neural network with a multi-layer structure⁴¹. The most important point is the parameters of ANFIS which must be optimized by other methods. In this study, the imperialist competitive algorithm (ICA) and the Firefly algorithm (FA) were used for optimization.

Firefly algorithm (FA). As an evolutionary algorithm, Firefly algorithm was first introduced by Yang in⁴². In recent years, many researchers have been using Firefly algorithm for optimization purposes⁴³. The results of this algorithm for solving optimization problems have been more satisfactory than other algorithms including SA, GA, PSO, and HAS⁴⁴. This meta-heuristic was inspired by firefly's flashing and their communication⁴². There are about 2000 firefly species, and most of them produce rhythmic and short flashes⁴⁵. Similar to other swarm intelligence algorithms whose details can capture a problem solution, in this algorithm each firefly is a solution to a problem. The light intensity also matches the objective function value. Notably, a firefly which has a brighter light is the solution and this firefly absorbs others.

Imperialist Competitive Algorithm (ICA). One of the novel evolutionary algorithms developed according to socio-political relations is the colonial competition, introduced originally by Atashpaz-Gargari and Lucas⁴⁶. Nowadays, ICA is known as a rich meta-heuristic algorithm and is used for optimization⁴⁷. As with other evolutionary algorithms, ICA is made up of a series of components each indicating a solution to problems trying to find the best solution. A general flowchart of flood susceptibility mapping can be seen in Fig. 9.

Evaluation and comparison methods. *Statistical error-index.* Evidently, when a new hybrid model is introduced, the performance of models should be evaluated and compared for both training and testing datasets. Basically, the results of modelling using a training dataset represent the degree of fit of models, while the results of a testing/validation dataset indicate the predictive power of modelling²⁸.

In this study, root mean square error (RMSE) and mean square error (MSE) were applied as statistical error evaluation criteria along with ROC curve for evaluating and comparing the performance of the two flood hybrid models. RMSE and MSE can be calculated as⁴⁸:

$$\text{RMSE} = \sqrt{\frac{\sum_{i=1}^n (X_{\text{est}} - X_{\text{obs}})^2}{N}} \quad (7)$$

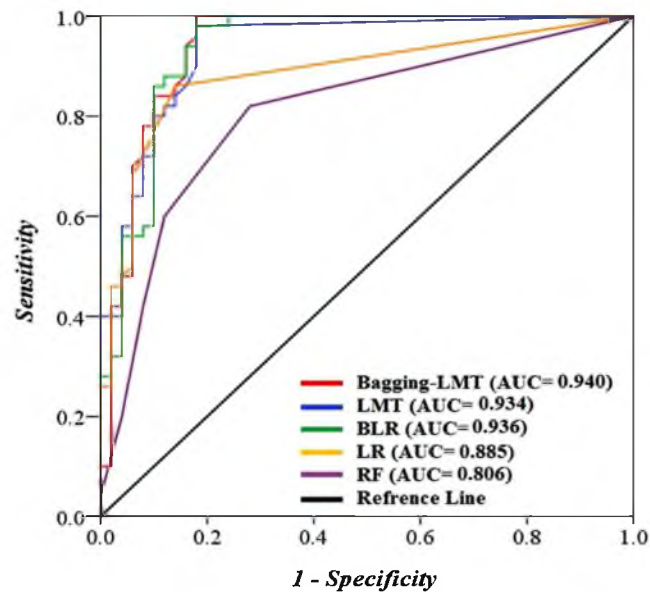


Figure 9. A general flowchart for optimization modelling in the study area.

$$\text{MSE} = \frac{1}{n} \sum_{i=1}^n (X_{\text{est}} - X_{\text{obs}})^2 \quad (8)$$

where, X_{est} denotes the value estimated by a model, X_{obs} is the actual value (observed), and n shows the number of observations in the dataset.

Receiver operating characteristic curve. Receiver Operating Characteristic (ROC) is another standard technique to determine the general performance of models, which has been used in geoscience⁴⁹. It is constructed by plotting the values of two statistical indexes, “sensitivity” and “100-specificity”, on the y-axis and x-axis, respectively⁵⁰. Based on the definition, the number of positive cases (flood) which are correctly classified as positive (flood) class refers to sensitivity, while 100-specificity is considered as the number of negative (non-flood) cases correctly classified as negative (non-flood) class.

The area under the ROC curve (AUROC) quantitatively evaluates the models’ performance and their capability of predicting an event’s occurrence or non-occurrence⁵¹. The AUROC represents how well a flood model generally performs. It ranges between 0.5 (inaccuracy) and 1 (perfect model/high accuracy), where the higher the AUROC, the better the model performance is⁵². The AUROC can be formulated as:

$$\text{AUROC} = \frac{\sum TP + \sum TN}{P + N} \quad (9)$$

where, TP refers to the percentage of positive instances which are classified correctly. TN shows the percentage of negative instances which are classified correctly. Then, P denotes the total number of events (flood), and N is the total number of no-events (non-flood).

Non-parametric statistical tests. The performance of the two new hybrid models for flood modelling was assessed by parametric and non-parametric statistical tests³. If the data follows a normal distribution with an equal variance, parametric methods are applied⁵³. Although non-parametric tests are free from any statistical assumptions, they are safer and their results are stronger than those of parametric tests, since the former do not assume normal distribution or homogeneity of variance⁵⁴. Since the conditioning factors have been classified as categorical classes, non-parametric statistical tests should be used. For this reason, Friedman⁵⁵ and Wilcoxon⁵⁶ sign rank tests were used to assess the differences between treatments of hybrid models. The objective of these tests was to reject or accept the null hypothesis stating that the performances of flood hybrid models were not different at the significance level of $\alpha = 0.05$ (or 5%).

The Friedman test was first used for the data to compare the significant differences between two or more models. Bui *et al.*⁵² reported that in the Friedman test, if p-value is less than 0.05, then the result is not applicable and we are not able to judge the significant differences between two or more models⁵². Therefore, the Wilcoxon signed-rank test was applied to specify the statistical significance of systematic pairwise differences between the two flood hybrid models using two criteria including p-value and the z-value. Eventually, the null hypothesis was rejected according to the p-value < 0.05 and z-value exceeding the critical values of z (-1.96 and $+1.96$). Accordingly, the performance of the susceptibility models differed significantly⁵².

References

- Zhou, Q., Leng, G. & Feng, L. Predictability of state-level flood damage in the conterminous United States: the role of hazard, exposure and vulnerability. *Scientific reports*. **7**, 5354 (2017).
- Moftakhari, H. R., Salvadori, G., AghaKouchak, A., Sanders, B. F. & Matthew, R. A. Compounding effects of sea level rise and fluvial flooding. *Proceedings of the National Academy of Sciences*. **114**, 9785–9790 (2017).
- Chapi, K. *et al.* A novel hybrid artificial intelligence approach for flood susceptibility assessment. *Environmental Modelling & Software*. **95**, 229–245 (2017).
- Zhao, Y., Xie, Q., Lu, Y. & Hu, B. Hydrologic Evaluation of TRMM Multisatellite Precipitation Analysis for Nanliu River Basin in Humid Southwestern China. *Scientific Reports*. **7**, 2470 (2017).
- Khosravi, K., Pourghasemi, H. R., Chapi, K. & Bahri, M. Flash flood susceptibility analysis and its mapping using different bivariate models in Iran: a comparison between Shannon's entropy, statistical index, and weighting factor models. *Environmental monitoring and assessment*. **188**, 656 (2016).
- Osati, K. *et al.* Spatiotemporal patterns of stable isotopes and hydrochemistry in springs and river flow of the upper Karkheh River Basin, Iran. *Isotopes in environmental and health studies*. **50**, 169–183 (2014).
- Chapi, K. *et al.* Spatial-temporal dynamics of runoff generation areas in a small agricultural watershed in southern Ontario. *Journal of Water Resource and Protection*. **7**, 14 (2015).
- Sarhadi, A., Soltani, S. & Modarres, R. Probabilistic flood inundation mapping of ungauged rivers: Linking GIS techniques and frequency analysis. *Journal of Hydrology*. **458**, 68–86 (2012).
- Rahmati, O., Pourghasemi, H. R. & Zeinivand, H. Flood susceptibility mapping using frequency ratio and weights-of-evidence models in the Golastan Province, Iran. *Geocarto International*. **31**, 42–70 (2016).
- Pradhan, B. Flood susceptible mapping and risk area delineation using logistic regression, GIS and remote sensing. *Journal of Spatial Hydrology*. **9** (2010).
- Rahman, R. & Saha, S. Remote sensing, spatial multi criteria evaluation (SMCE) and analytical hierarchy process (AHP) in optimal cropping pattern planning for a flood prone area. *Journal of Spatial Science*. **53**, 161–177 (2008).
- Kazakis, N., Kougias, I. & Patsialis, T. Assessment of flood hazard areas at a regional scale using an index-based approach and Analytical Hierarchy Process: Application in Rhodope–Evros region, Greece. *Science of the Total Environment*. **538**, 555–563 (2015).
- Tehrany, M. S., Pradhan, B. & Jebur, M. N. Flood susceptibility mapping using a novel ensemble weights-of-evidence and support vector machine models in GIS. *Journal of hydrology*. **512**, 332–343 (2014).
- Rahmati, O. & Pourghasemi, H. R. Identification of Critical Flood Prone Areas in Data-Scarce and Ungauged Regions: A Comparison of Three Data Mining Models. *Water Resources Management*. **31**, 1473–1487 (2017).
- Cao, C. *et al.* Flash flood hazard susceptibility mapping using frequency ratio and statistical index methods in coalmine subsidence areas. *Sustainability*. **8**, 948 (2016).
- Mukerji, A., Chatterjee, C. & Raghuvanshi, N. S. Flood forecasting using ANN, neuro-fuzzy, and neuro-GA models. *Journal of Hydrologic Engineering*. **14**, 647–652 (2009).
- Kia, M. B. *et al.* An artificial neural network model for flood simulation using GIS: Johor River Basin, Malaysia. *Environmental Earth Sciences*. **67**, 251–264 (2012).
- Shafizadeh-Moghadam, H., Valavi, R., Shahabi, H., Chapi, K. & Shirzadi, A. Novel forecasting approaches using combination of machine learning and statistical models for flood susceptibility mapping. *Journal of environmental management*. **217**, 1–11 (2018).
- Tehrany, M. S., Pradhan, B., Mansor, S. & Ahmad, N. Flood susceptibility assessment using GIS-based support vector machine model with different kernel types. *Catena*. **125**, 91–101 (2015).
- Jothibasu, A. & Anbazhagan, S. Flood Susceptibility Appraisal in Ponnaiyar River Basin, India using Frequency Ratio (FR) and Shannon's Entropy (SE) Models. *International Journal of Advanced Remote Sensing and GIS*, 1946–1962 (2016).
- Khosravi, K. *et al.* A comparative assessment of decision trees algorithms for flash flood susceptibility modeling at Haraz watershed, northern Iran. *Science of The Total Environment*. **627**, 744–755 (2018).
- Liu, R. *et al.* Assessing spatial likelihood of flooding hazard using naive Bayes and GIS: a case study in Bowen Basin, Australia. *Stochastic environmental research and risk assessment*. **30**, 1575–1590 (2016).
- Wang, Z. *et al.* Flood hazard risk assessment model based on random forest. *Journal of Hydrology*. **527**, 1130–1141 (2015).
- Nayak, P., Sudheer, K., Rangan, D. & Ramasastri, K. Short-term flood forecasting with a neurofuzzy model. *Water Resources Research*. **41** (2005).
- Bui, D. T. *et al.* Hybrid artificial intelligence approach based on neural fuzzy inference model and metaheuristic optimization for flood susceptibility modeling in a high-frequency tropical cyclone area using GIS. *Journal of Hydrology*. **540**, 317–330 (2016).
- Ayalew, L. & Yamagishi, H. The application of GIS-based logistic regression for landslide susceptibility mapping in the Kakuda-Yahiko Mountains, Central Japan. *Geomorphology*. **65**, 15–31 (2005).
- Akgun, A., Sezer, E. A., Nefeslioglu, H. A., Gokceoglu, C. & Pradhan, B. An easy-to-use MATLAB program (MamLand) for the assessment of landslide susceptibility using a Mamdani fuzzy algorithm. *Computers & Geosciences*. **38**, 23–34 (2012).
- Bui, D. T., Pradhan, B., Lofman, O., Revhaug, I. & Dick, O. B. Spatial prediction of landslide hazards in Hoa Binh province (Vietnam): a comparative assessment of the efficacy of evidential belief functions and fuzzy logic models. *Catena*. **96**, 28–40 (2012).
- Lee, S. Comparison of landslide susceptibility maps generated through multiple logistic regression for three test areas in Korea. *Earth Surface Processes and Landforms*. **32**, 2133–2148 (2007).
- Hong, H. *et al.* Spatial prediction of landslide hazard at the Luxi area (China) using support vector machines. *Environmental Earth Sciences*. **75**, 40 (2016).
- García-Davalillo, J. C., Herrera, G., Notti, D., Strozzi, T. & Álvarez-Fernández, I. DInSAR analysis of ALOS PALSAR images for the assessment of very slow landslides: the Tena Valley case study. *Landslides*. **11**, 225–246, <https://doi.org/10.1007/s10346-012-0379-8> (2014).
- Daniel, C. 131 Note: on varying one factor at a time. *Biometrics*. **14**, 430–431 (1958).
- Daniel, C. One-at-a-time plans. *Journal of the American statistical association*. **68**, 353–360 (1973).
- Ilija, I. & Tsangaratos, P. Applying weight of evidence method and sensitivity analysis to produce a landslide susceptibility map. *Landslides*. **13**, 379–397 (2016).
- Kersulienė, V., Zavadskas, E. K. & Turskis, Z. Selection of rational dispute resolution method by applying new step-wise weight assessment ratio analysis (SWARA). *Journal of Business Economics and Management*. **11**, 243–258 (2010).
- Zengqiang, M., Cunzhi, P. & Yongqiang, W. In *Control Conference*, 2008. CCC 2008. 27th Chinese. 554–558 (IEEE).
- Jang, J.-S. ANFIS: adaptive-network-based fuzzy inference system. *IEEE transactions on systems, man, and cybernetics*. **23**, 665–685 (1993).
- Shirzadi, A. *et al.* A comparative study between popular statistical and machine learning methods for simulating volume of landslides. *Catena*. **157**, 213–226 (2017).
- Khashei-Siuki, A. & Sarbazi, M. Evaluation of ANFIS, ANN, and geostatistical models to spatial distribution of groundwater quality (case study: Mashhad plain in Iran). *Arabian Journal of Geosciences*. **8**, 903–912 (2015).
- Celikyilmaz, A. & Turksen, I. B. Modeling uncertainty with fuzzy logic. *Studies in fuzziness and soft computing*. **240**, 149–215 (2009).
- Ahmadlou, M. *et al.* Flood susceptibility assessment using integration of adaptive network-based fuzzy inference system (ANFIS) and biogeography-based optimization (BBO) and BAT algorithms (BA). *Geocarto International*. 1–21 (2018).
- Yang, X.-S. *Nature-inspired metaheuristic algorithms*. (Luniver press, 2010).

43. Yeomans, J. S. In *Intelligence Systems in Environmental Management: Theory and Applications* 207–229 (Springer, 2017).
44. Alweshah, M. & Abdullah, S. Hybridizing firefly algorithms with a probabilistic neural network for solving classification problems. *Applied Soft Computing*. **35**, 513–524 (2015).
45. Zeng, Y., Zhang, Z. & Kusiak, A. Predictive modeling and optimization of a multi-zone HVAC system with data mining and firefly algorithms. *Energy*. **86**, 393–402 (2015).
46. Atashpaz-Gargari, E. & Lucas, C. In *IEEE Congress on Evolutionary Computation*. 4661–4667 (2007).
47. Coelho, L. D. S., Afonso, L. D. & Alotto, P. A modified imperialist competitive algorithm for optimization in electromagnetics. *IEEE Transactions on Magnetics*. **48**, 579–582 (2012).
48. Shirzadi, A. *et al.* Shallow landslide susceptibility assessment using a novel hybrid intelligence approach. *Environmental Earth Sciences*. **76**, 60 (2017).
49. Shahabi, H., Khezri, S., Ahmad, B. B. & Hashim, M. Landslide susceptibility mapping at central Zab basin, Iran: a comparison between analytical hierarchy process, frequency ratio and logistic regression models. *Catena*. **115**, 55–70 (2014).
50. Shahabi, H. & Hashim, M. Landslide susceptibility mapping using GIS-based statistical models and Remote sensing data in tropical environment. *Scientific reports*. **5**, 9899 (2015).
51. Yesilnacar, E. & Topal, T. Landslide susceptibility mapping: a comparison of logistic regression and neural networks methods in a medium scale study, Hendek region (Turkey). *Engineering Geology*. **79**, 251–266 (2005).
52. Bui, D. T., Tuan, T. A., Klempe, H., Pradhan, B. & Revhaug, I. Spatial prediction models for shallow landslide hazards: a comparative assessment of the efficacy of support vector machines, artificial neural networks, kernel logistic regression, and logistic model tree. *Landslides*. **13**, 361–378 (2016).
53. D'Arco, M., Liccardo, A. & Pasquino, N. ANOVA-based approach for DAC diagnostics. *IEEE Transactions on Instrumentation and Measurement*. **61**, 1874–1882 (2012).
54. Derrac, J., García, S., Molina, D. & Herrera, F. A practical tutorial on the use of nonparametric statistical tests as a methodology for comparing evolutionary and swarm intelligence algorithms. *Swarm and Evolutionary Computation*. **1**, 3–18 (2011).
55. Friedman, M. The use of ranks to avoid the assumption of normality implicit in the analysis of variance. *Journal of the American statistical association*. **32**, 675–701 (1937).
56. Wilcoxon, F. Individual comparisons by ranking methods. *Biometrics bulletin*. **1**, 80–83 (1945).

Acknowledgements

This research was financially supported by Iran National Science Foundation (INSF) through the research project No. 96004000, International Partnership Program of Chinese Academy of Sciences (Grant No. 115242KYSB20170022), Universiti Teknologi Malaysia (UTM) based on Research University Grant (QJ130000.2527.17H84), and also we would like to thanks Samaneh Kansar Zamin (SKZ) company for funding the research and providing access to their nationwide geodatabase.

Author Contributions

D.T.B., M.P., H.S., V.P.S., A.S., K.C., K.K., W.C., S.P., S.L. and B.B.A. contributed equally to the work. H.S., A.S. and W.C. collected field data and conducted the flood mapping and analysis. M.P., H.S., A.S., K.C., K.K. and W.C. wrote the manuscript. D.T.B., V.P.S., S.P. S.L. and B.B.A., provided critical comments in planning this paper and edited the manuscript. All the authors discussed the results and edited the manuscript.

Additional Information

Competing Interests: The authors declare no competing interests.

Publisher's note: Springer Nature remains neutral with regard to jurisdictional claims in published maps and institutional affiliations.



Open Access This article is licensed under a Creative Commons Attribution 4.0 International License, which permits use, sharing, adaptation, distribution and reproduction in any medium or format, as long as you give appropriate credit to the original author(s) and the source, provide a link to the Creative Commons license, and indicate if changes were made. The images or other third party material in this article are included in the article's Creative Commons license, unless indicated otherwise in a credit line to the material. If material is not included in the article's Creative Commons license and your intended use is not permitted by statutory regulation or exceeds the permitted use, you will need to obtain permission directly from the copyright holder. To view a copy of this license, visit <http://creativecommons.org/licenses/by/4.0/>.

© The Author(s) 2018